Geophysical Research Letters

RESEARCH LETTER
10.1029/2019GL082374

Elevation Drives Gradients in Surface Soil Temperature Within Salt Marshes

Merryl Alber[1] and **Jessica L. O'Connell**[1]

[1]Department of Marine Sciences, University of Georgia, Athens, GA, USA

Key Points:
- Surface soil temperature exhibits spatial variability within salt marshes and is inversely correlated with elevation on the marsh platform
- Satellite estimates of surface temperature exhibit these same relationships at broader scales
- We know little about how small-scale variability in soil temperature affects rates of salt marsh processes

Supporting Information:
- Supporting Information S1

Correspondence to:
M. Alber,
malber@uga.edu

Citation:
Alber, M., & O'Connell, J. L. (2019). Elevation drives gradients in surface soil temperature within salt marshes. *Geophysical Research Letters*, *46*, 5313–5322. https://doi.org/10.1029/2019GL082374

Received 5 FEB 2019
Accepted 29 APR 2019
Accepted article online 6 MAY 2019
Published online 27 MAY 2019

Abstract Elevation differences in salt marshes result in numerous ecological consequences as a result of variation in tidal flooding. We demonstrate here that elevation differences are also negatively correlated with soil temperature on the marsh platform, irrespective of tidal flooding. Field observations of soil temperature at 10-cm depth in a Georgia marsh showed that elevation increases of 0.5 m corresponded to decreases in average soil temperature of 0.9–1.7°C during both winter and summer. Landsat 8 estimates of land surface temperatures across the marsh in dry (nonflooded) scenes also showed that temperature decreased with increasing elevation, which was consistent with soil observations. Similar satellite results were also found in a test marsh in Virginia. Biological reactions are temperature-dependent, and these findings indicate that metabolic processes will vary over short distances. This is important for accurately estimating marsh metabolism and predicting how changes in temperature will affect future productivity.

1. Introduction

Salt marshes are valuable ecosystems that store carbon, provide habitat for both aquatic and terrestrial organisms, serve as sites of chemical transformation, and protect the shore (Barbier et al., 2011). Although marshes occur in low-lying areas with little topographic relief (generally less than 2 m; McKee & Patrick, 1988), elevation is a critical variable in these systems and even small differences in elevation can affect the flow of water as it moves across the landscape. Gradients in inundation have been shown to influence soil salinity and moisture (Adams, 1963), nutrient availability (Mitsch & Gosselink, 2000), aeration (Chapman, 1974), and redox potential (Mendelssohn & Morris, 2000) in tidal marshes. Elevation differences are also associated with the characteristic distribution of height forms of the salt marsh cord grass, *Spartina alterniflora* (Hladik et al., 2013; Mendelssohn & Morris, 2000), which is taller when it occurs adjacent to creeks than when it is found on the marsh platform (e.g., the midmarsh area where the ground is firmer). Although soil temperature also plays an important role in marsh metabolism and plant growth, to our knowledge, temperature variability along marsh elevation gradients has not been investigated previously.

Most studies that have evaluated the effects of temperature on salt marsh processes focus on large temporal and spatial scales. For example, there have been numerous studies comparing seasonal or latitudinal differences in factors such as sulfate reduction (Koretsky et al., 2003), plant productivity (Kirwan et al., 2009), organic matter decay (Kirwan et al., 2014), and CO_2 emission (Morris & Whiting, 1986). Although within-site variability may be small compared to that observed at larger scales, the implicit assumption is that marsh soil temperatures are homogenous and do not vary in a spatially predictable way at fine scales. Moreover, investigators often rely on a limited number of sampling locations (e.g., Kirwan et al., 2014; Morris & Whiting, 1986) and/or use air temperature to characterize environmental conditions (e.g., Angermeyer et al., 2018; Wieski & Pennings, 2014). Here we present evidence that soil temperature varies systematically with small elevation differences within a salt marsh, with potential consequences for temperature dependent ecosystem processes.

2. Methods

2.1. Study Site

This study was conducted in a *S. alterniflora* marsh in the intertidal area of the Duplin River on Sapelo Island, GA, USA. The site is within the Georgia Coastal Ecosystems Long-Term Ecological Research (GCE-LTER) domain and is adjacent to the GCE eddy covariance flux tower (lat: 31.441°, long: -81.284°, https://gce-lter.marsci.uga.edu). The water table is typically high at this site, and soils are fairly saturated,

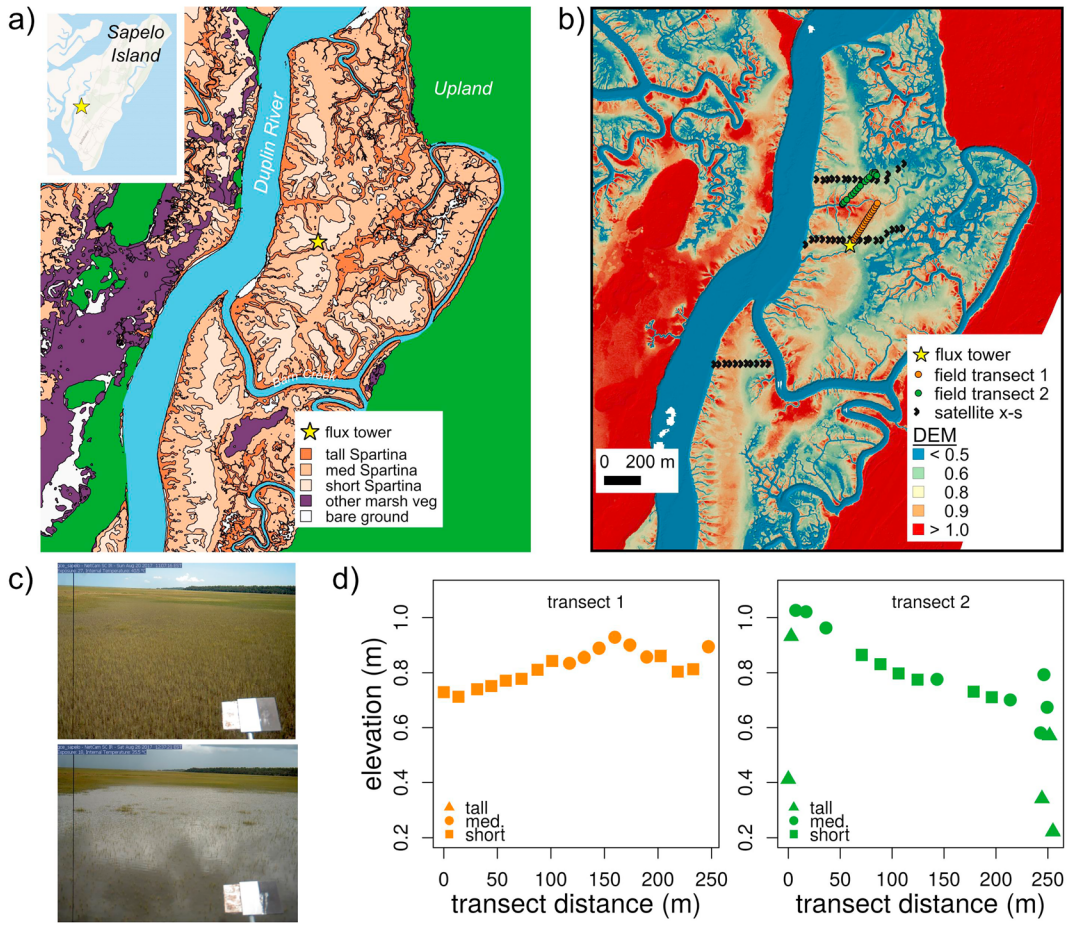

Figure 1. Characteristics of the study area, which is located in a tidal marsh off the Duplin River, adjacent to Sapelo Island, GA, USA. (a) Vegetation classification, showing areas of short, medium, and tall form *S.alterniflora* as well as the location of the Georgia Coastal Ecosystems Long-Term Ecological Research (GCE-LTER) flux tower. Inset shows location of the study site on Sapelo Island, GA. (b) Digital elevation model (DEM), in m relative to NADV 88, including the locations of the two field transects (circles) and the satellite cross sections (x-s, shown as > symbol) used in this study. (c) Example images from the "GCESapelo" PhenoCam during dry (top) and flooded (bottom) conditions. The PhenoCam is located on the flux tower and looks to the NE across transect 1. (d) Elevations at tidbit locations along field transect 1 (left) and 2 (right), beginning at the southernmost point in each case. Symbols denote *Spartina alterniflora* height form at each location.

even at low tide. Marsh vegetation along the Duplin River was mapped by Hladik et al. (2013) and consists of >88% *S. alterniflora*, with tall-form plants (classified as plants >1.0 m in height) found close to tidal channels and a mix of medium (0.5–1.0 m) and short (<0.5 m) plants in the marsh interior (Figure 1a). They found that plants categorized as tall *S. alterniflora* occurred at an average elevation of 0.36 m, whereas plants categorized as medium and short were at average elevations of 0.77 and 0.87 m, respectively (all elevations are relative to NAVD88; Figure 1b; Hladik & Alber, 2012). The marsh platform at this site ranges between 0.5 and 1.1 m and has a median elevation of 0.8 m (C. Burns, pers. comm.). Tides are semidiurnal with a range of ~1.2 m on the marsh platform.

The GCE eddy covariance flux tower has a suite of ancillary sensors that collect information at 5-min interval year-round. This includes measurements of temperature in the air (~1 m above the flux tower platform), soil (~10 m into the marsh interior from the tower, integrated between 5 and 10 cm), and water (measured in a tidal creek just south of the tower by a pressure transducer that also records water level). Temperature records from 2013 to 2018 (Figure S2 in the supporting information) show that soil temperature is warmer than either creek water or air, with mean daily soil temperature ranging from 13.1°C in winter to 28.0°C in summer as compared to winter means of 12.1 and 11.7°C and summer means of 27.7 and 26.7°C for

Table 1
Mean and Range of Soil Temperatures (°C) in Dry and Flooded Conditions as Measured During Field Deployments of Tidbit Temperature Probes

		Dry temp (°C)		Flooded temp (°C)	
Deployment	Dates	Mean	Range	Mean	Range
Transect 1	27 July to 31 August 2017	12.5	1.5	11.2	1.7
Transect 1	8 January to 13 February 2018	28.9	1.1	28.4	1.1
Transect 2	23 August to 18 September 2018				
>0.5 m		28.7	1.1	28.9	0.9
<0.5 m		28.9	0.3	28.9	0.2

Note. All observations in transect 1 were >0.5 m in elevation. Transect 2 results are separated by elevation ranges. Transect locations are shown in Figure 1.

water and air, respectively. Note that differences between soil and air temperature are larger in winter than in summer. The "GCESapelo" PhenoCam (StarDot NetCam SC 5MP IR, StarDot Technologies) is mounted on the tower and collects oblique images of the study marsh every half-hour during daylight (Figure 1c).

2.2. Field Measurements

We used tidbit temperature probes (HOBO UA-002-08, Onset Computer Corp) buried 10 cm into the soil to measure soil temperature in the study marsh during three different deployments. The first two deployments were along a transect that began just to the north of the eddy covariance flux tower (Figure 1b). The transect ran 247 m northeast toward the edge of a tidal creek, with a total of 18 probes placed every 14 m. This transect was entirely on the marsh platform, covering an elevation range of 0.7 to 0.9 m, and vegetation was a mix of medium and short form *S. alterniflora* (Figure 1d). Tidbits recorded soil temperature every 15 min for approximately 1-month periods in summer and winter (Table 1). For the third deployment we set up a second transect in which we placed probes strategically in low-lying areas as well as on top of the natural levee in order to expand the range of elevation covered by the observations (Figure 1d). The transect, which was conducted in summer (Table 1), ran 255 m and spanned an elevation range of 0.2 to 1.0 m. Vegetation at the beginning and end of the transect was tall *S. alterniflora*, with a mix of height forms at the other locations. The positions and elevations of stations occupied during both deployment locations were geo-referenced with a Trimble R6 real time kinematic Global Positioning System receiver with submeter vertical and horizontal accuracy.

Soil temperature observations were separated into flooded or dry conditions based on creek water heights recorded by a pressure transducer associated with the flux tower. Marsh flooding is not a straightforward function of creek water height and can vary with respect to wind direction, wind speed, and other parameters. However, we know definitively when the marsh was flooded in areas near the PhenoCam, which photographs the marsh condition every 30 min (Figure 1c), and based on these observations, we derived cutoffs for creek water level that we could use to confidently assign probe status as either flooded or dry (O'Connell et al., 2017; O'Connell & Alber, 2016). We designated conditions as flooded when creek water height was >0.2 m above the probe elevation and dry when the creek water was <0.2 m below the probe and set all other observations as unknown flood status. We then reduced each temperature probe data set to the mean of all observations during flooded and dry conditions over the course of the deployment.

The relationship between soil temperature, elevation, and flooding status on the marsh platform for each of the three deployments was evaluated by fitting linear models of the form temperature = elevation * flood status for elevations > 0.5 m. This included observations from the full set of 18 tidbits from each of the first two deployments and 15 of the 18 tidbits from the third deployment. Tidbits at elevations <0.5 m were deployed in unconsolidated mud, and temperatures had a different relationship with elevation and a different response to flooding in these areas (see results).

2.3. Satellite Measurements

Landsat 8 was used to estimate land surface temperature patterns on the marsh platform in order to evaluate the robustness of the relationship between elevation and soil temperature observed in field transects. This

analysis was limited to dry conditions because we were interested in evaluating marsh surface temperature, which is obscured during flooded conditions.

We preprocessed Landsat imagery, which has 30- × 30-m pixels, to obtain cloud-free low-tide observations for all available Landsat 8 scenes (Mar 2013 through Oct 2018). The pixel_qa band from the Landsat 8 surface reflectance product was used to filter out cloudy pixels. Low tide scenes were then identified through the combined use of the PhenoCam, which was used to estimate the degree of marsh flooding during the hours that Landsat passed over the site (see O'Connell & Alber, 2016), and the creek water height sensor, which was used to filter out scenes where creek water was above 0.5 m, as this is above the height of the marsh platform, and so we can assume it was flooded. We identified 10 winter (January and February) and 11 summer (August and September) scenes for downstream analysis, selected to correspond with our field observation periods. Two of these (5 February 2018 and 20 August 2017) were used as examples to visualize land surface temperature variation during winter and summer, respectively.

Land surface temperature was estimated based on band 10 top of atmosphere brightness temperature (wavelength midpoint at 10.9 μm), as provided in the Landsat 8 surface reflectance product (landsat.usgs.gov/landsat-8). We did not use Band 11, also a thermal band, because noise from stray light makes correcting this band to surface temperature difficult (Cook et al., 2014). Band 10 was converted to land surface temperature with a radiative transfer equation (supporting information), which Yu et al. (2014) identified as giving the most accurate results for Landsat 8. The mean elevation of each pixel was estimated from a 1-m^2 digital elevation model created for our study area, which was vertically corrected to account for vegetation interference (Hladik & Alber, 2012). At the Landsat scale, marsh pixels with elevations < 0.5 m contained mixed cover of marsh and creeks, and so we limited our analyses to pixels >0.5 m. It would be interesting to evaluate lower elevation areas, but that would require finer spatial resolution thermal bands than we had available in order to separate creeks from low elevation marsh.

Generalized additive models (GAMs) were used to formally evaluate the relationship between land surface temperature and mean pixel elevation (supporting information). Data for this analysis were based on three cross sections that started at the Duplin River and proceeded east through *S. alterniflora* marsh until dense or large tidal creeks were encountered (Figure 1b). Surface temperatures from these cross sections were obtained for all available Landsat winter and summer scenes, which were modeled separately. GAMs are useful because they account for nonlinear relationships between the response variable and the predictors through the use of smoothing functions (Wood, 2017).

2.3.1. Additional Test Case

The remote sensing approach outlined above can be used to derive land surface temperatures for comparison with marsh elevation at other sites. As a test case, we applied our workflow to winter scenes from a *Spartina*-dominated salt marsh located in the Virginia Coast Reserve LTER to evaluate whether the temperature-elevation relationship was similar to what we observed in Georgia (supporting information). Note that the marsh platform sits lower in the tidal frame at this site as compared to that in Georgia, and so the lowest elevation included in the analysis was 0.3 rather than 0.5 m (relative to NAVD 88).

3. Results

3.1. Field Results

Soil temperature varied with elevation in all three deployments of the tidbit temperature probes. This was true even though elevation did not steadily decrease from the marsh interior to the creek edge (Figure 1d). Temperature along the first transect, adjacent to the flux tower, was inversely related to elevation during both summer and winter deployments, spanning a range of 1.1 to 1.7°C depending on conditions (Table 1). Slopes in temperature elevation relationships were steeper in winter than summer (Figures 2a and 2b), which may be because the temperature deficit between air and soil was greater in winter (Figure S2). In the third deployment, which occurred during summer along the second transect, temperature was again inversely related to elevation for observations above 0.5 m, with a slope and range similar to that observed during the summer deployment along the other transect (Figure 2c). In contrast, temperature remained relatively constant at elevations below 0.5 m.

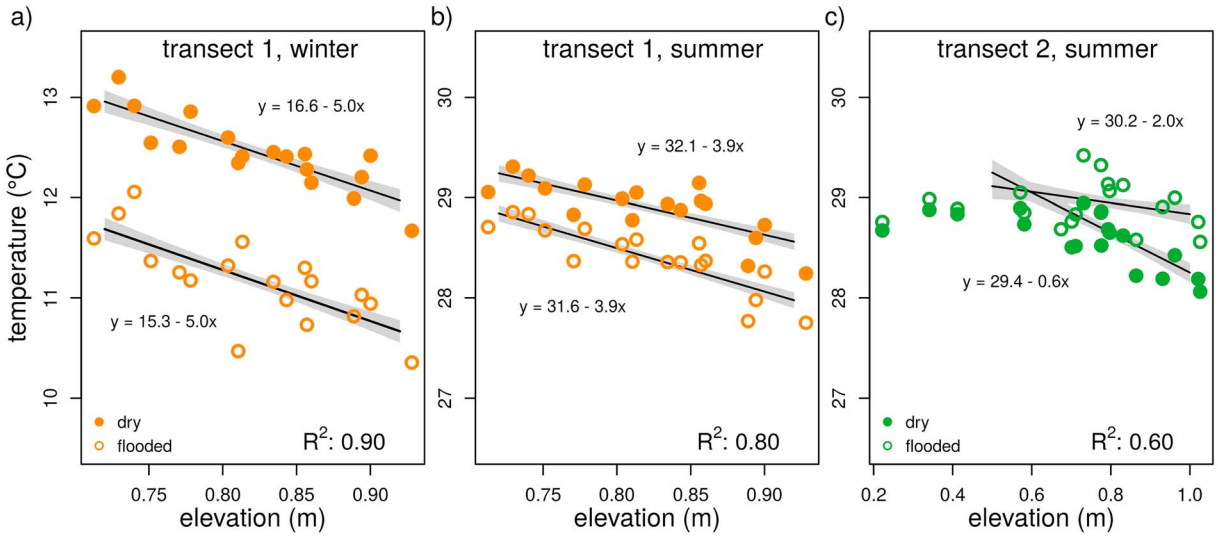

Figure 2. Mean soil temperature versus elevation measured at 10-cm depth along (a) transect 1 during winter, (b) transect 1 during summer, and (c) transect 2 during summer in the GA study area. Dry (closed circles) and flooded (open circles) conditions are plotted separately. Linear models for flooded and dry observations >0.5 m are shown (solid lines) along with confidence intervals (dotted lines) and line equations. The R^2 for linear models of the form temperature = elevation * flood status is shown for each deployment.

Flooding had differential effects on soil temperatures in the two field transects. In the transect adjacent to the flux tower flooding had a cooling effect: mean soil temperature decreased from 12.5 to 11.2°C in winter and from 28.9 to 28.4 °C in summer during flooding as compared to dry conditions (Table 1). This was likely due to the fact that the water in the estuary, which was brought in with the tide, was cooler than the soil (the average temperature of creek water adjacent to the flux tower was 12.2 and 28.1°C during the first two deployments). In the second transect flooding resulted in fairly homogeneous temperatures along the entire elevation gradient. During flooded conditions, the average temperature of the tidbits located on the marsh platform increased slightly, from 28.7 to 28.9°C. This was unexpected, as average temperature of the flux tower creek water was again cooler than the soil during this deployment (28.3°C) and suggests that there was a source of warmer water that flooded this marsh area. We speculate that ponding of warmer water in low elevation areas close to the upland may influence flood water temperatures in this area. In contrast, flooding had no effect on soil temperature in areas <0.5 m, which averaged 28.9°C during both flooded and dry conditions. This suggests that low elevation areas close to tidal creeks remain saturated throughout the tidal cycle.

Linear models that included both elevation and flooding were able to explain a large portion of the variation in daily mean soil temperature at elevations >0.5 m during all three deployments (R^2 ranged from 0.60 to 0.90; Figure 2). However, dry conditions were much more common than completely flooded marsh conditions; 83% of the observations included in the analysis were from dry conditions. Moreover, elevation had a stronger influence on temperature than flooding: the monthly mean temperatures during the three deployments ranged by 1.1–1.5°C during dry conditions and flooding changed these ranges by < 0.2°C (Table 1). Thus, the elevation response during dry conditions was the dominant driver of the marsh temperature regime.

3.2. Satellite Results

Landsat 8 surface temperature varied across the marsh in a similar manner to that observed in the field transects. Surface temperatures in the estuary and the tidal creeks were cooler than temperatures on the marsh surface during both winter and summer (Figure 3a), which is similar to flux tower records that showed that water temperature was typically cooler than soil temperature year round (Figure S2). However, surface temperatures were slightly warmer than soil temperatures during both summer and winter. Landsat 8 passed over our site at ~16:00 UTC, which corresponded to 11:00 am EST, and so it is not surprising that temperatures were warmer at the surface than at 10-cm depth. When we focused on *S.*

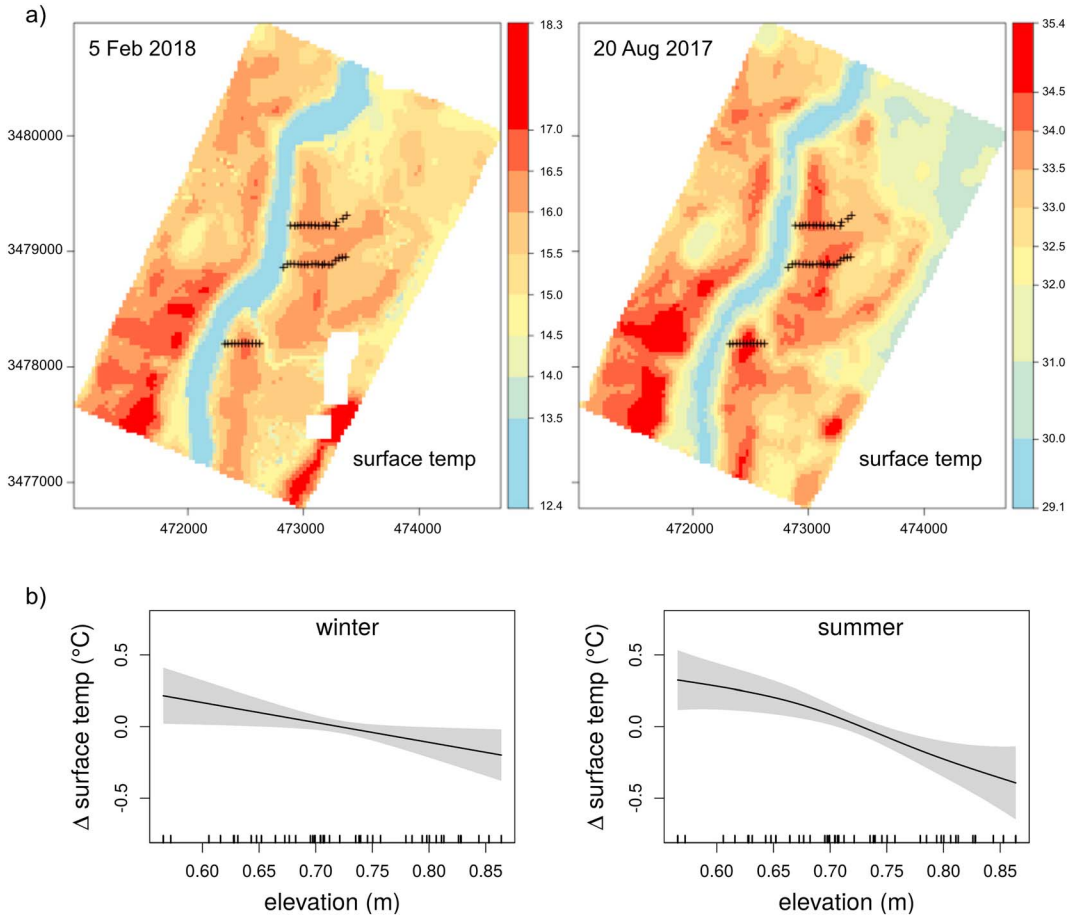

Figure 3. Landsat 8 surface temperature during low tide conditions on (a) 5 February 2018 (left) and 20 August 2017 (right) in the GA study area. Locations of the cross sections used for analysis are denoted by plus signs (see also Figure 1b). The color ramp for each image denotes °C and is scaled to maximize within-image variation by setting the minimum value on that date as blue and the maximum value as red. Thus, colors between images do not represent the same temperature. (b) Landsat 8 surface temperature change versus elevation estimated from Generalized Additive Models for winter (left) and summer (right) during dry conditions across all three satellite cross sections, based on 10 and 11 scenes, respectively. The solid lines are the best fit lines; the shaded grey areas show the 95% confidence interval. Internal lines along the *x* axis represent a rug plot that shows the distribution of observations.

alterniflora marsh areas at elevations >0.5 m, we found that land surface temperatures varied even more broadly than soil temperatures, spanning a range of 3°C in winter (13.9 to 17°C on 5 February 2018) and almost 4°C in summer (31.0 to 34.9°C on 20 August 2017). Patterns were similar to those observed in the field transects, with cooler temperatures in areas of higher elevation (compare Figure 1a with Figure 3a).

The GAMs (Equation S7), which included all available winter and summer Landsat 8 observations, explained 63% of the temperature change in winter and 84% in summer, and in both cases the elevation relationship was significant ($p = 0.03$ and $p < 0.001$, respectively). The elevation-temperature relationship again trended downward as elevation increased (Figure 3b). Thus patterns in Landsat land surface temperature during dry (low tide) conditions mirrored the field-collected data. The expected values from the models (e.g., the best fit lines) had a smaller range than that observed on individual cross-sections because these values represented the mean tendency from dates spanning multiple years and months, which averaged out observed extremes. However, land surface temperature variability on individual days was still quite dynamic (Figure 3a).

3.2.1. Additional Test Case

Satellite analysis of the Virginia test site supported the trends we observed in Georgia (Figure 4). Elevation across three cross sections ranged from 0.3 to 0.7 m, and over four winter dates the change in land surface

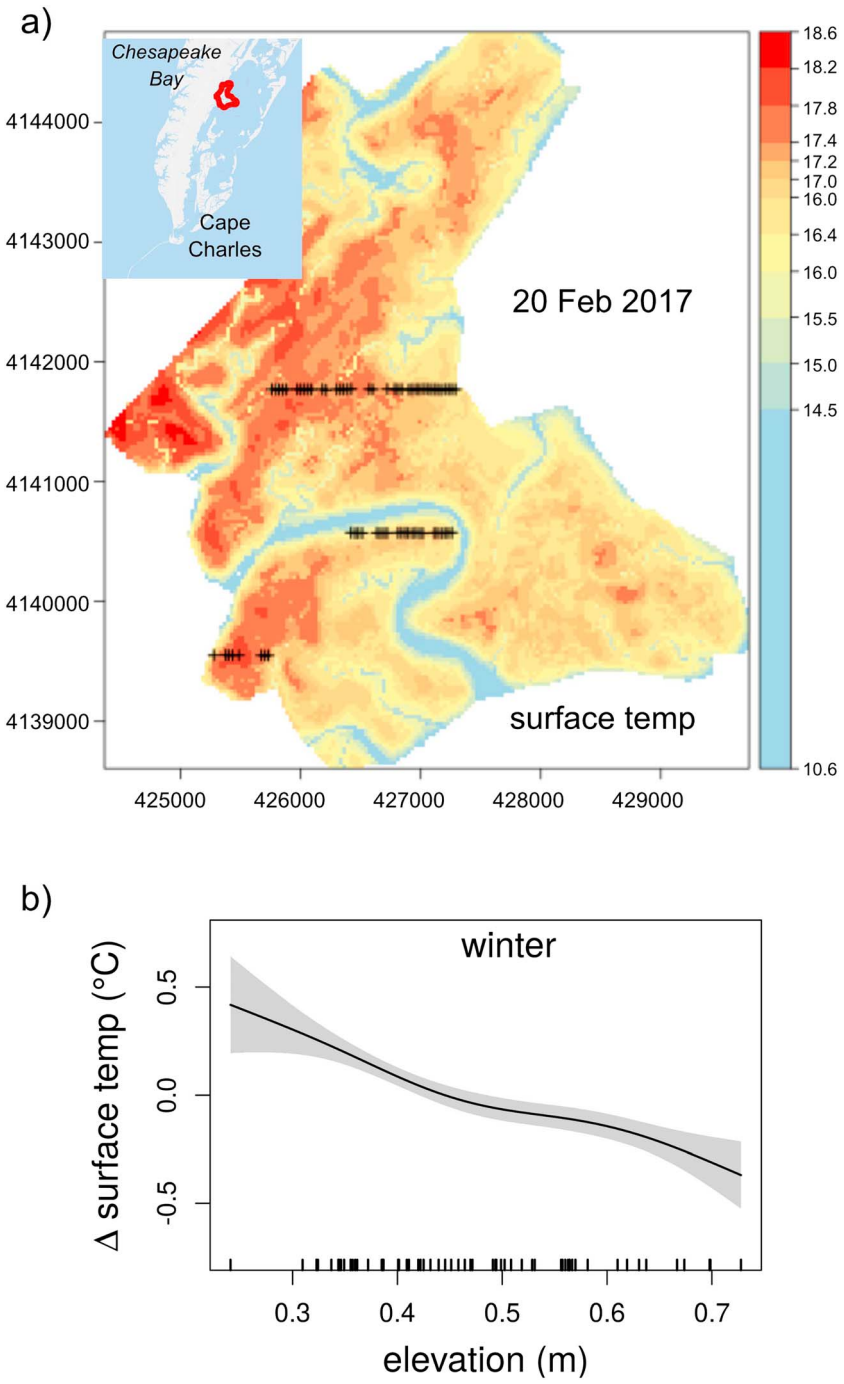

Figure 4. Landsat 8 analysis in the VA test marsh (a) surface temperature during low tide conditions on 20 February 2017, with locations of the cross-sections used for analysis denoted by plus signs. (Inset shows location on the eastern shore of Chesapeake Bay). (b) Landsat 8 surface temperature change versus elevation estimated from Generalized Additive Model across all three satellite cross sections, based on four scenes during winter. The solid lines are the best fit lines; the shaded grey areas show the 95% confidence interval. Internal lines along the *x* axis represent a rug plot that shows the distribution of observations.

temperature spanned an average of 0.9°C and was as high as 1.3°C. The GAM explained 60% of the variation in temperature change, and the elevation-temperature relationship was negative and significant ($p < 0.001$).

4. Discussion and Conclusions

This study demonstrated that soil temperature varied over small elevation gradients within salt marshes, with differences of 0.9–1.7 °C across plots located only tens of meters apart. This was supported by Landsat 8-based surface temperature estimates, which showed negative relationships with elevation at our primary study site in Georgia as well as a test case in Virginia. Although surface temperatures are not a perfect proxy for soil temperatures, Piccolo et al. (1993) showed that temperatures within the top 10 cm of a mudflat responded rapidly to changes in surface temperature. The response dampened with depth, with little variation in sediment temperature at 25 cm. The consistency in our field and Landsat-based results suggests that surface temperatures derived from satellites, coupled with a digital elevation model, can serve as a useful tool for examining spatial patterns in marsh temperature.

Intertidal soil temperatures are typically influenced by heat exchange with surface temperature of both air and water (Piccolo et al., 1993; Seybold et al., 2002), but the mechanism for the inverse relationship between elevation and temperature observed on the marsh platform is unknown. Ewing (1986) observed a 2–8°C difference in soil temperature among brackish marsh sites in Puget Sound, WA, where he also reported an elevation difference of 1.4 m, which is consistent with our observations. However, air temperatures in mangroves have been shown to be cooler in concave topographic depressions (Osland et al., 2019; Ross et al., 2009), which are not typically observed in salt marshes. It would be therefore be instructive to investigate these relationships in a variety of marshes with different climate and flooding regimes as well as different wetland types.

A classic paradigm in salt marsh ecology is that the action of the tidal flushing results in a cascade of environmental differences that influence plant distribution: tidal waters carry oxygen, boosting root metabolism; they carry nutrients, fertilizing plants; and they help to flush potential toxins from the pore water, such as salt, root metabolites, and hydrogen sulfide (King et al., 1982; Mendelssohn & Morris, 2000). The temperature-elevation relationship we observed on the marsh platform, where the majority of the plants are located, is fundamentally different because it was not driven by the tide. This is in keeping with Silvestri et al. (2005), who suggested that soil water flow is independent of tidal flooding. Thus, gradients in soil temperature, although keyed to topographic differences, occur regardless of tidal flooding patterns on the marsh platform. We only had a few observations in low-lying areas, but they showed that soil temperatures had a constant temperature regime regardless of elevation or flooding, suggesting that soil temperatures were buffered compared to those on the marsh platform. Interestingly, these tend to be very wet areas at the creek edge where tall *S. alterniflora* is usually found.

Soil temperature regimes are important because biological reactions are temperature-dependent. If we assume a Q10 of 2, for example, then a 0.9 –1.7°C change in temperature as observed in our field transects would result in a 6-12% difference in the rate of a reaction (following the Arrhenius equation). This suggests that the rates of soil processes ranging from nutrient cycling (e.g., denitrification, nitrification, and sulfate reduction) to plant growth (e.g., primary production and CO_2 emission) to infaunal and microbial activity (e.g., soil respiration and decomposition) are likely to vary substantially across a salt marsh. Temperature will also affect physical characteristics such as salt accumulation (and therefore soil salinity; Wang et al., 2007). Microspatial differences in soil temperature caused by elevation gradients will also have consequences for understanding vegetation growth patterns and for modeling *S. alterniflora* productivity, as rates of gross production, dark respiration, and organic matter decomposition are all temperature-dependent. For example, cooler soils associated with higher elevations on the marsh platform may play a part in slowing *S. alterniflora* root growth and the timing of shoot initiation compared with plants in low-lying areas. We are currently exploring whether differences in soil growing degree days can explain variation in the date of spring green-up across this marsh.

These findings have implications for changing climate patterns, as spatial heterogeneity in soil temperature suggests that not all parts of the marsh will respond similarly to the same event. Based on our findings, we predict that droughts and heat waves should have a harsher effect in low-lying areas where soil temperatures are warmer. This is consistent with our observations of drought-associated marsh dieback, which can occur in low-lying areas. Freezes are extremely rare at this study site, but we would predict that higher elevations would be more susceptible to late spring freezes than lower elevations as soils are already cooler. The effects of sea level rise on temperature gradients are unclear given the complex feedbacks between plant

production, elevation, and sediment trapping (Fagherazzi et al., 2012). However, if changes in elevation affect soil temperature and hence plant production that will influence a marsh's ability to accrete vertically. Temperatures are also increasing worldwide and are expected to increase further (USGCRP, 2017), which again may affect marsh metabolism and plant growth patterns differentially depending on elevation. Thus, this study highlights the importance of incorporating temporal and spatial variation in soil temperature into our understanding of coastal marshes and invites a reconsideration of marsh metabolism.

Acknowledgments
This research was supported by NSF (Georgia Coastal Ecosystems LTER OCE12-37140, OCE18-32178, and Coastal SEES NSF14-26308). We thank Rick Peterson for the loan of the tidbit temperature probes, Christine Burns for information on the Virginia study marsh, and Dontrece Smith, Alyssa Peterson, Jacob Shalack and Peter Hawman for help with field data collection. Soil temperature observations (http://gce-lter.marsci.uga.edu/data/MSH-GCED-1904) and Landsat cross-section data (http://gce-lter.marsci.uga.edu/data/MSH-GCE0-1904) are available through the GCE data catalog. DEM data for GA are from Hladik et al. (2013) and are available through GCE (https://doi.org/10.6073/pasta/4c5187ef603f70cd0a77ece24ef0fed9); those for VA are through VCR (https://www.vcrlter.virginia.edu/gisdata/LIDAR/USGS2015/). Raw Landsat scenes are available at earthexplorer.usgs.gov. This is contribution 1078 of the University of Georgia Marine Institute.

References

Adams, D. A. (1963). Factors influencing vascular plant zonation in North Carolina salt marshes. *Ecology*, *44*(3), 445–456. https://doi.org/10.2307/1932523

Angermeyer, A., Crosby, S. C., & Huber, J. A. (2018). Salt marsh sediment bacterial communities maintain original population structure after transplantation across a latitudinal gradient. *PeerJ*, *6*, e4735. https://doi.org/10.7717/peerj.4735

Barbier, E. B., Hacker, S. D., Kennedy, C., Koch, E. W., Stier, A. C., & Silliman, B. R. (2011). The value of estuarine and coastal ecosystem services. *Ecological Monographs*, *81*(2), 169–193. https://doi.org/10.1890/10-1510.1

Chapman, V. J. (1974). *Salt Marshes and Salt Deserts of the World*. Lehre, Germany: J. Cramer. https://doi.org/10.1016/B978-0-12-586450-3.50006-8

Cook, M., Schott, J. R., Mandel, J., & Raqueno, N. (2014). Development of an operational calibration methodology for the Landsat thermal data archive and initial testing of the atmospheric compensation component of a Land Surface Temperature (LST) product from the archive. *Remote Sensing*, *6*(11), 11,244–11,266. https://doi.org/10.3390/rs61111244

Ewing, K. (1986). Plant growth and productivity along complex gradients in a Pacific Northwest brackish intertidal marsh. *Estuaries*, *9*(1), 49–62. https://doi.org/10.2307/1352193

Fagherazzi, S., Kirwan, M. L., Mudd, S. M., Guntenspergen, G. R., Temmerman, S., D'Alpaos, A., et al. (2012). Numerical models of salt marsh evolution: Ecological, geomorphic, and climatic factors. *Reviews of Geophysics*, *50*, RG1002. https://doi.org/10.1029/2011RG000359

Hladik, C., & Alber, M. (2012). Accuracy assessment and correction of a LIDAR-derived salt marsh digital elevation model. *Remote Sensing of Environment*, *121*, 224–235. https://doi.org/10.1016/j.rse.2012.01.018

Hladik, C., Schalles, J., & Alber, M. (2013). Salt marsh elevation and habitat mapping using hyperspectral and LIDAR data. *Remote Sensing of Environment*, *139*, 318–330. https://doi.org/10.1016/j.rse.2013.08.003

King, G. M., Klug, M. J., Wiegert, R. G., & Chalmers, A. G. (1982). Relation of soil water movement and sulfide concentration to *Spartina alterniflora* production in a Georgia salt marsh. *Science*, *218*(4567), 61–63. https://doi.org/10.1126/science.218.4567.61

Kirwan, M. L., Guntenspergen, G. R., & Langley, L. A. (2014). Temperature sensitivity of organic-matter decay in tidal marshes. *Biogeosciences*, *11*(17), 4801–4808. https://doi.org/10.5194/bg-11-4801-2014

Kirwan, M. L., Guntenspergen, G. R., & Morris, J. T. (2009). Latitudinal trends in *Spartina alterniflora* productivity and the response of coastal marshes to global change. *Global Change Biology*, *15*(8), 1982–1989. https://doi.org/10.1111/j.1365-2486.2008.01834.x

Koretsky, C. M., Moore, C. M., Lowe, K. L., Meile, C., DiChristina, T. J., & van Capellen, P. (2003). Seasonal oscillation of microbial iron and sulfate reduction in saltmarsh sediments. *Biogeochemistry*, *64*(2), 179–203. https://doi.org/10.1023/A:1024940132078

McKee, K. L., & Patrick, W. H. Jr. (1988). The relationship of smooth cordgrass (*Spartina alterniflora*) to tidal datums: A review. *Estuaries*, *11*(3), 143–151. https://doi.org/10.2307/1351966

Mendelssohn, I. A., & Morris, J. T. (2000). Eco-physiological controls on the productivity of *Spartina alterniflora* Loisel. In M. P. Weinstein & D. A. Kreeger (Eds.), *Concepts and Controversies in Tidal Marsh Ecology*, (pp. 59–80). Dordrecht, Netherlands: Springer. https://doi.org/10.1007/0-306-47534-0_5

Mitsch, W. J., & Gosselink, J. G. (2000). *Wetlands*. New York: John Wiley.

Morris, J. T., & Whiting, G. J. (1986). Emission of gaseous carbon dioxide from salt-marsh sediments and its relation to other carbon losses. *Estuaries*, *9*(1), 9–19. https://doi.org/10.2307/1352188

O'Connell, J. L., & Alber, M. (2016). A smart classifier for extracting environmental data from digital image time-series: Applications for PhenoCam data in a tidal salt marsh. *Environmental Modelling & Software*, *84*, 134–139. https://doi.org/10.1016/j.envsoft.2016.06.025

O'Connell, J. L., Mishra, D. R., Cotten, D. L., Wang, L., & Alber, M. (2017). The Tidal Marsh Inundation Index (TMII): An inundation filter to flag flooded pixels and improve MODIS tidal marsh vegetation time-series analysis. *Remote Sensing of Environment*, *201*, 34–46. https://doi.org/10.1016/j.rse.2017.08.008

Osland, M. J., Hartmann, A. K., Day, R. H., Ross, M. S., Hall, C. T., & Vervaeke, W. C. (2019). Microclimate influences mangrove freeze damage: Implications for range expansion in response to changing macroclimate. *Estuaries and Coasts*, *42*(4), 1084–1096. https://doi.org/10.1007/s12237-019-00533-1

Piccolo, M. C., Perillo, G. M. E., & Daborn, G. R. (1993). Soil temperature variations on a tidal flat in Minas Basin, Bay of Fundy, Canada. *Estuarine, Coastal and Shelf Science*, *36*, 345–357. https://doi.org/10.1006/ecss.1993.1021

Ross, M. S., Ruiz, P. L., Sah, J. P., & Hanan, E. J. (2009). Chilling damage in a changing climate in coastal landscapes of the subtropical zone: A case study from south Florida. *Global Change Biology*, *15*(7), 1817–1832. https://doi.org/10.1111/j.1365-2486.2009.01900.x

Seybold, C. A., Mersie, W., Huang, J., & McNamee, C. (2002). Soil redox, pH, temperature, and water-table patterns of a freshwater tidal wetland. *Wetlands*, *22*(1), 149–158. https://doi.org/10.1672/0277-5212(2002)022[0149:SRPTAW]2.0.CO;2

Silvestri, S., Defina, A., & Marani, M. (2005). Tidal regime, salinity and salt marsh plant zonation. *Estuarine, Coastal and Shelf Science*, *62*(1-2), 119–130. https://doi.org/10.1016/j.ecss.2004.08.010

USGCRP (2017). In D. J. Wuebbles, D. W. Fahey, K. A. Hibbard, D. J. Dokken, B. C. Stewart, & T. K. Maycock (Eds.), *Climate Science Special Report: Fourth National Climate Assessment*. Washington, DC: U.S. Global Change Research Program. https://doi.org/10.7930/J0J964J6

Wang, H., Hsieh, Y. P., Harwell, M. A., & Huang, W. (2007). Modeling soil salinity distribution along topographic gradients in tidal salt marshes in Atlantic and Gulf coastal regions. *Ecological Modelling*, *201*(3-4), 429–439. https://doi.org/10.1016/j.ecolmodel.2006.10.013

Wieski, K., & Pennings, S. C. (2014). Climate drivers of *Spartina alterniflora* saltmarsh production in Georgia, USA. *Ecosystems*, *17*(3), 473–484. https://doi.org/10.1007/s10021-013-9732-6

Wood, S. N. (2017). *Generalized Additive Models: An Introduction with R* (2nd ed.). Boca Raton, Florida: Chapman & Hall/CRC. https://doi.org/10.1201/9781315370279

Yu, X., Guo, X., Wu, Z., Yu, X., Guo, X., & Wu, Z. (2014). Land surface temperature retrieval from Landsat 8 TIRS—Comparison between radiative transfer equation-based method, split window algorithm and single channel method. *Remote Sensing*, *6*, 9829–9852. https://doi.org/10.3390/rs6109829